UDK 62-4:669.018.25:004.032.26
Original scientific article/Izvirni znanstveni članek

ISSN 1580-2949
MTAEC9, 50(6)851(2016)

MODELING OF SHOT-PEENING EFFECTS ON THE SURFACE PROPERTIES OF A (TiB + TiC)/Ti–6Al–4V COMPOSITE EMPLOYING ARTIFICIAL NEURAL NETWORKS

MODELIRANJE VPLIVA HLADNEGA POVRŠINSKEGA KOVANJA NA LASTNOSTI POVRŠINE (TiB + TiC)/Ti-6Al-4V KOMPOZITA S POMOČJO UMETNIH NEVRONSKIH MREŽ

Erfan Maleki, Abolghassem Zabihollah

Sharif University of Technology, International Campus, Department of Mechanical Engineering, Kish Island, 7941776655, Iran
maleki_erfan@kish.sharif.edu, maleky.erfan@gmail.com

Prejem rokopisa – received: 2015-06-29; sprejem za objavo – accepted for publication: 2015-11-13

doi:10.17222/mit.2015.140

Titanium matrix composites (TMCs) have wide application prospects in the field of aerospace, automobile and other industries because of their good properties, such as high specific strength, good ductility, and excellent fatigue properties. However, in order to improve their fatigue strength and life, crack initiation and growth at the surface layers must be suppressed using surface treatments. Shot peening (SP) is an effective surface mechanical treatment method widely used in industry which can improve the mechanical properties of a surface. However, artificial neural networks (ANNs) have been used as an efficient approach to predict and optimize the science and engineering problems. In the present study the effects of SP on TMC were modeled by means of ANN and the capability of the ANN in predicting the output parameters is investigated. A back-propagation (BP) error algorithm is developed for the network training. Data of experimental tests on the (TiB + TiC)/Ti–6Al–4V composite are employed in order to train the network. The volume fractions of the reinforcements (TiB + TiC) were 5 % and 8 %. ANN testing is accomplished using different experimental data thaat were not used during the network training. The distance from the surface (depth) and SP intensity are regarded as input parameters and residual stress and hardness of the Ti–6Al–4V before and after the SP and adding reinforcements are gathered as the output parameters of the network. A comparison was made between experimental and predicted data. The predicted results were in good agreement with experimental ones, which indicates that developed neural network can be used for modeling the SP process on TMCs.

Keywords: titanium matrix composites, surface treatment, shot peening, artificial neural networks, residual stress, hardness

Kompoziti na osnovi titana (TMCs) imajo široko možnost uporabe na področju letalstva, avtomobilske in druge industrije zaradi njihovih dobrih lastnosti, kot so: velika specifična trdnost, dobra duktilnost in odlična odpornost na utrujanje. Vseeno pa je za povečanje odpornosti na utrujanje in življenjsko dobo, potrebna površinska obdelava, da se zavre nastanek razpok in njihova rast na površini. Hladno površinsko kovanje (SP) je učinkovita mehanska metoda, ki se v industriji pogosto uporablja za izboljšanje mehanskih lastnosti površine. Umetne nevronske mreže (ANNs) se uporabljajo kot učinkovit približek za napovedovanje in optimiranje znanstvenih osnov in inženiringa tega problema. V študiji so bili modelirani vplivi SP na TMC s pomočjo ANN in preiskovana je bila zmožnost napovedovanja izhodnih parametrov z ANN. Za usposabljanje mreže je bil razvit algoritem vzvratnega širjenja napak (BP). Podatki iz eksperimentalnih preizkusov na (TiB + TiC)/Ti–6Al–4V kompozitu so uporabljeni za usposabljanje mreže. Volumska deleža delcev (TiB + TiC) za ojačanje sta bila 5 % in 8 %. ANN preizkušanje je bilo izvedeno z uporabo različnih eksperimentalnih podatkov, ki niso bili uporabljeni pri usposabljanju mreže. Razdalja od površine (globina) in intenziteta SP sta uporabljeni kot vhodna parametra, preostala, napetost in trdota Ti–6Al–4V, pred in po SP, in dodatku delcev za ojačanje, sta izbrana kot izhodna parametra mreže. Izvedena je bila primerjava med eksperimentalnimi in predvidenimi podatki. Predvideni rezultati so se dobro ujemali z eksperimentalnimi, kar kaže na to, da se razvito nevronsko mrežo lahko uporabi pri modeliranju SP postopka na TMC.

Ključne besede: kompoziti na osnovi titana, obdelava površine, hladno kovanje površine, umetna nevronska mreža, zaostale napetosti, trdota

1 INTRODUCTION

Titanium matrix composites (TMCs) have attracted considerable interest due to their attractive properties over titanium alloys, such as high elastic modulus, high strength, superior creep and fatigue resistances at ambient and elevated temperatures.[1–4] The fabrication of TMCs using in-situ technology is simple and does not result in the pollution of an interface.[5,6] TMCs can be reinforced with continuous fibers, whiskers or particles.[7] As is well known, the mechanical properties of the composites depend on matrix, reinforcement and reinforcement/matrix interface, which bonds the formers together.[8] Compared with continuous fibers, TMCs reinforced with whiskers or particles exhibit more isotropic behaviors. The fabrication of these materials is more convenient and cost effective; therefore, they have drawn extensive attention recently.[9] Titanium monoboride (TiB) whiskers and titanium carbide (TiC) particles offer high modulus, relative chemical stability, and high thermal stability, while maintaining similar density and thermal expansion coefficient to those of the titanium matrix, as well as clean interfaces without any unfavorable reaction between the precipitates and the titanium matrix.[10–12] The

reinforcements were obtained according to the high-temperature reactions as follows in Equations (1) and (2):[13,14]

$$5Ti+B4C = 4TiB+TiC \quad (1)$$

$$Ti+C = TiC \quad (2)$$

TMCs co-reinforced with TiB whiskers and TiC particles have been fabricated and investigated for their mechanical properties[15–17] and have been extensively demonstrated to possess superior mechanical properties over the single TiB or TiC reinforced discontinuously reinforced titanium matrix composites (DRTMCs).[18–21]

As an effective and important surface-treatment method, shot peening (SP) can introduce high residual compressive stress (RCS) and microstructure variation at near surface layers, which can enhance their fatigue properties compared to non-peened materials. The process of SP involves the bombardment of spherical balls of a hard material against the surface of components, which induces the strong elastic–plastic deformation at the surface and sub-surface regions. In the deformation layers, high RCS and microstructure refinements are introduced after SP. The residual stresses and hardness are very important properties of materials after the SP treatment.

In the field of science and engineering, artificial neural networks (ANNs) are some of the most important research areas. ANN is a modeling tool to solve linear and nonlinear multivariate regression problems.[22] Recently, ANN models were widely utilized to interpret and correlate the variable relationships in complex nonlinear data sets. The present study proposes a new approach based on ANNs to investigate the effects of SP process on mechanical and metallurgical properties (TiB + TiC)/Ti–6Al–4V composite. Residual stress and hardness were modeled by ANN. 20 data of experimental tests results from the total of 30, are used to train the networks, while in the networks testing 10 different experimental data which were not used during training are used. Since the experimental results did not include the training sets the performance of the ANN is evaluated in a fine way.

2 EXPERIMENTAL PART

The experimental data are obtained from Xie et al.[23] The materials of (TiB + TiC)/Ti–6Al–4V (TiB:TiC = 1:1 (vol.%)) were fabricated via in-situ technology. Two types of theoretical total volume fraction of reinforcements (TiB + TiC) were 5 % and 8 %. The SP treatment was performed using an air-blast machine. The related information of used SP process is demonstrated in **Table 1**. The Almen specimens are A type and the diameter of peening nozzle was 15 mm and the distance between nozzle and sample was 100 mm. In order to obtain the depth distribution of the residual stress and hardness, the thin top surface layers were removed one by one via the method of chemical etch with a solution of water, nitric acid, and hydrofluoric acid in the ratio 31:12:7. All the measurements were carried out at room temperature. The method of residual stress and hardness measurements are X ray stress analysis and digital microhardness test respectively.[23]

Table 1: Parameters of the SP process treatments[23]
Tabela 1: Parametri uporabljenega procesa SP[23]

SP intensity (mm A)	Shot material	Shot diameter (mm)	Shot hardness (HV)	Jet pressure (MPa)	SP time (min)	Coverage (%)
0.15	Cast steel	0.6	610	0.2	0.50	100
0.30	Cast steel	0.6	610	0.3	0.50	100

The results indicate that the increased reinforcements and SP intensities enhance the surface roughness after SP. Both the compressive residual stresses and hardness increase with the increase of the SP intensity, which is mainly due to the plastic deformation and high dislocation density in the near surface layer. Moreover, the reinforcement particles can act as the block sources during dislocation movements. After an appropriate SP treatment, the increased CRS and hardness are beneficial to industrial applications A table shows the obtained values of the experimental results on (TiB + TiC)/Ti–6Al–4V for 30 different samples. The SP intensity for non-peened specimens has been shown by zero in **Table 2**.

3 ARTIFICIAL NEURAL NETWORKS

Artificial intelligence (AI) systems such as artificial neural networks (ANNs) have found many applications in science and engineering problems in the past decade. The concept of an ANN has emerged with the idea that it

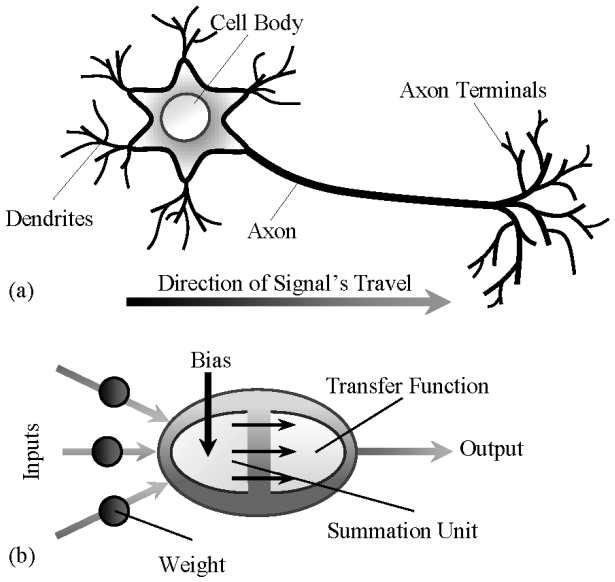

Figure 1: Schematic of neuron: a) a biological neuron, b) an artificial neuron
Slika 1: Shematski prikaz nevrona: a) biološki nevron, b) umetni nevron

Table 2: Values of the SP process effects on residual stress and hardness of (TiB + TiC)/Ti–6Al–4V Composite specimens[23]
Tabela 2: Vrednosti SP postopka, ki vplivajo na zaostale napetosti in trdoto (TiB + TiC) / Ti-6Al-4V kompozitnih vzorcev[23]

Sample No.	Depth	SP intensity (mm A)	Residual Stress (MPa)			Hardness (HV)		
			matrix	5 % (TIB+TIC)	8 % (TIB+TIC)	matrix	5 % (TIB+TIC)	8 % (TIB+TIC)
1	0	0.00	10.42	18.04	17.93	334.72	380.37	417.57
2	0	0.30	-522.83	-524.25	-575.51	524.87	560.38	637.31
3	0	0.15	-375.97	-434.55	-481.94	484.31	512.07	584.43
4	15	0.00	25.11	5.022	6.84	328.67	393.61	436.62
5	15	0.30	-613.76	-648.62	-657.79	436.11	512.19	628.86
6	15	0.15	-417.53	-499.54	-539.63	418.45	492.85	523.28
7	25	0.00	-9.57	-20.26	-12.97	325.48	381.28	420.16
8	25	0.30	-608.67	-650.57	-672.54	414.97	468.23	557.85
9	25	0.15	-408.92	-465.67	-574.80	387.62	451.56	507.09
10	50	0.00	14.35	-29.48	-9.19	315.39	403.32	411.77
11	50	0.30	-581.27	-608.46	-626.77	378.62	455.55	530.79
12	50	0.15	-397.63	-419.90	-545.84	372.53	431.43	475.18
13	75	0.00	14.48	14.02	-12.72	338.28	381.40	423.67
14	75	0.30	-564.84	-570.02	-586.49	385.38	438.64	538.40
15	75	0.15	-354.00	-386.95	-516.88	358.29	420.55	446.63
16	100	0.00	-12.84	-17.01	-14.41	340.03	396.67	414.43
17	100	0.30	-557.53	-524.25	-515.10	368.47	433.57	509.66
18	100	0.15	-324.71	-337.52	-264.28	349.94	411.35	459.31
19	150	0.00	-5.26	-11.81	-8.67	330.01	375.66	409.48
20	150	0.30	-422.37	-335.69	-299.08	350.72	388.76	438.64
21	150	0.15	-302.74	-249.65	-120.90	340.80	386.23	435.87
22	200	0.00	16.96	-13.89	-4.75	319.14	386.77	429.04
23	200	0.30	-323.74	-220.36	-101.37	354.10	402.29	434.42
24	200	0.15	-236.84	-194.73	-61.16	344.29	382.99	424.21
25	250	0.00	28.21	14.93	17.41	337.86	375.06	424.09
26	250	0.30	-46.11	-20.82	-28.14	343.11	380.31	428.50
27	250	0.15	-31.80	-18.99	-15.97	336.83	378.90	410.87
28	300	0.00	-13.62	-23.50	21.33	344.74	369.26	414.91
29	300	0.30	-35.15	-18.99	-33.63	324.51	381.15	430.88
30	300	0.15	-18.99	-11.67	-16.23	326.86	376.50	419.41

simulates the operating principles of a human brain. The first studies were made with mathematical modeling of biological neurons that make up the brain cells.[24] Basically, the brain functions with a very dense network of neurons. The brain contains a lot of neurons connected to each other by many interconnections. A neuron consists mainly of the following parts: dendrite, cell body and axon.[25] Dendrite gets the signals from various other neurons to the neuron and carries them to the cell body for processing, after that an axon carries the signal from the cell body to various other neurons. Similarly, the neural units in the artificial neural network are developed as a very approximate model of the natural biological neurons.[26] **Figure 1** shows a natural biological neuron (**Figure 1a**) and an artificial neuron (**Figure 1b**) that is a computational and mathematical model of the biological neuron. A single neuron computes the sum of its inputs, which are multiplying with a variant called the weight, adds a bias term, and drives the result through a generally nonlinear transfer function to produce a single output termed the activation level of the neuron.

An ANN model is created by interconnection of many of the neurons in a known configuration. The primary elements characterizing the neural network are the distributed representation of information, local operations and non-linear processing. Structurally, every ANN is made up of three sections: input, hidden and output layers.[27] The structure of an ANN model is determined by the number of its layers and the number of nodes in each layer and the nature of the transfer function.[28,29] Selecting the optimum architecture of the network is one of the challenging steps in ANN modeling. The term "architecture" refers to the number of layers in the network and the number of neurons in each layer. However, there is no straightforward method to estimate the optimal number of hidden layers and neurons in each layer.[30,31] Thus trial-and-error methods have been used by many researchers to determine such case-dependent parameters for studies involving ANN-based models.[32] **Figure 2** represents the architecture of the neural network. In this network, each input consists of *r* parameters and each output comprises *s* parameters,

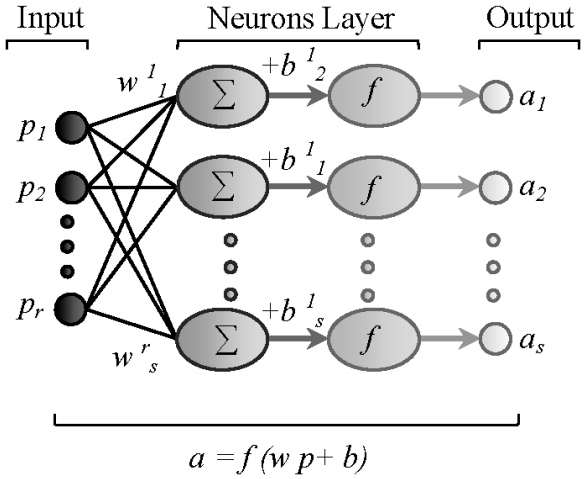

Figure 2: Architecture of neural network[33]
Slika 2: Zgradba nevronske mreže[33]

while p, w, b, f and a represent the inputs, weight matrixes, bias vectors, transfer function in neurons, and outputs, respectively.[33]

Mathematically, a layer n may be described by Equations (3) and (4):[34]

$$u_s^n = \sum_{i=1}^{r} w_s^n p_i \tag{3}$$

$$a_s = f(v_s^n) = f(u_s^n + b_s^n) \tag{4}$$

where p_1, p_2, . . ., p_r are the input signals, $w^k{}_1$, $w^k{}_2$, . . ., $w^n{}_s$ are the synaptic weights of neuron n, u^n is the linear combiner output due to input signals, b^n is the bias, f is the transfer function and a_1, a_2, . . ., a_s are the output signals of the neuron. The tangent sigmoid (Tansig) $\phi(x)$, logarithmic sigmoid (Logsig) $\psi(x)$ and linear $\chi(x)$ transfer function are described as follows in Equations (5), (6) and (7):[35]

$$\phi(x) = \frac{2}{1+e^{-2x}} - 1 \tag{5}$$

$$\psi(x) = \frac{2}{1+e^{-x}} \tag{6}$$

$$\chi(x) = linear(x) \tag{7}$$

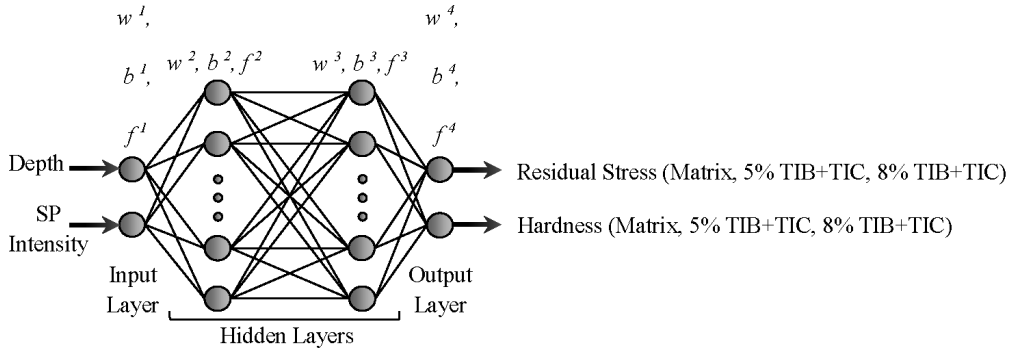

Figure 3: A Conceptual structure of network with four layers
Slika 3: Konceptualna zgradba mreže s štirimi nivoji

3.1 Training of ANN

The training of the ANN is performed by adjusting the connection weights. It is performed by iteratively adjusting the weights (w) of the connections and biases (b) in the network in order to minimize a predefined cost function.[36] The ANNs are trained with a training set of input and known output data. An ANN is better trained as more input data are used. The performance of an ANN is generally based on the parameters' architecture and the setting. As was mentioned, one of the most difficult tasks in studying ANNs is finding an appropriate architecture. This task is performed via trial and error and the number of middle layers and neuron presented in each layer is being identified. Appropriate designation of the initial amounts of weights and biases is very effective on the performance of network and the time of calculation. But there is not a reasonable law and process to identify a suitable architecture. The only step which is very time consuming is the trial and error. One can get an idea by looking at a problem and decide to start with simple networks; going on to complex ones until the solution is within acceptable limits of uncertainty. Furthermore, the point that must be considered in training of the network is the rate of input and output data scattering. In this study all values of each input and output data parameters are divided to maximum absolute value of them and normalized also the used data are dimensionless. The normalized data are in range of [–1, +1]. In the present study, a feed forward ANN based on back propagation (BP) error algorithm, which is the most popular one in training of ANNs is used. BP is a descent algorithm, which attempts to minimize the error during iterations. The weights of the network are adjusted by the algorithm such that the error is decreased along a descent direction. In the back-propagation learning, the actual outputs are compared with the target values to derive the error signals, which are propagated backward layer by layer for the updating of the synaptic weights in all the lower layers.

3.2 Implementation of ANN

In this paper the effects of the SP process on surface properties including of (TiB + TiC) / Ti–6Al–4V composite were modeled by means of an ANN. In implementation of the ANN distance from the surface (depth) and SP intensity are regarded as inputs and the residual stress and hardness are gathered as outputs of the networks. Different networks with different architecture and network parameters were trained for the prediction of residual stress and hardness. **Figure 3**, for an example, represents the schematic architecture of ANN for modeling of the mentioned output parameters: a four-layer feed forward with BP algorithm with full interconnection. This neural network model has a powerful input-output mapping capability. With the use of enough hidden neurons, it can effectively approximate any continuous nonlinear function. In the considered network, two inputs are logged into the input layer to determine the two outputs. In the ANN methodology, the sample data is often subdivided into training and testing sets. The distinctions among these subsets are crucial.[37] Ripley defines the following: Training set: a set of examples used for learning that is to fit the parameters of the classifier. Testing set: a set of examples used only to assess the performance of a fully-specified classifier.

3.3 Performance evaluation of ANN

The performance of the ANN models in predicting the shot-peening effects on residual stress and hardness of (TiB + TiC)/Ti–6Al–4V composite were statistically evaluated using four prediction score metrics calculated from the test dataset: Pearson coefficient of correlation (PCC), root mean square error (RMSE), mean relative error (MRE) and mean absolute error (MAE). These parameters were determined using the following Equations (8), (9), (10) and (11):

$$PCC=\frac{\sum_{i=1}^{n}(f_{EXP,i}-F_{EXP})-(f_{ANN,i}-F_{ANN})}{\sqrt{\sum_{i=1}^{n}(f_{EXP,i}-F_{EXP})^2-(f_{ANN,i}-F_{ANN})^2}} \quad (8)$$

$$RMSE=\sqrt{\frac{\sum_{i=1}^{n}(f_{EXP,i}-f_{ANN})^2}{n}} \quad (9)$$

$$MRE=\frac{1}{n}\sum_{i=1}^{n}\frac{\left|f_{EXP,i}-f_{ANN,1}\right|}{f_{EXP,i}}\times 100 \quad (10)$$

$$MRE=\frac{1}{n}\sum_{i=1}^{n}\left|f_{EXP,i}-f_{ANN,1}\right| \quad (11)$$

where n is the number of used sample for modeling, f_{EXP} is the experimental value and f_{ANN} is the networks predicted value. Also, the values of F_{EXP} and F_{ANN} are calculating as follows in Equations (12) and (13):

$$F_{EXP}=\frac{1}{n}\sum_{i=1}^{n}f_{EXP,i} \quad (12)$$

$$F_{ANN}=\frac{1}{n}\sum_{i=1}^{n}f_{ANN,i} \quad (13)$$

3.4 Generating model function

After the neural network is trained successfully with four layers, the values of the four parameters of the network (p, b, w and f) can be obtained. The function that correlates the inputs to the corresponding output can be calculated by applying the aforementioned parameters. Finally, the model function can determined in Equations (14) and (15):

$$a^1=f^1(w^1p+b^1) \quad (14a)$$

$$a^2=f^2(w^2p^1+b^2) \quad (14b)$$

$$a^3=f^3(w^3p^2+b^3) \quad (14c)$$

$$a^4=f^4(w^4p^3+b^4) \quad (14d)$$

$$G\,(g(1),\,g(2))=a^4= \\ =f^4(w^4f^3\,(w^{3\,2}(w^2f^1(w^1p+b^1)+\,b^2)\,+b^3)+\,b^4) \quad (15)$$

where a^1, a^2 and a^3 are the outputs of the first, second and third layer, respectively; a^4 is the fourth layer output, which is equal to the function G ($g(1)$, $g(2)$). The function G gets the values of the input parameters. The function of $g(1)$and $g(2)$ represent the residual stress and hardness, respectively. The methodology used for neural network application in this study is as follows:

1. Start;
2. Normalize the data (inputs & outputs);
3. Feed the data to artificial neural network;
4. Find network optimum parameters;
5. Execute network training;
6. Obtain Pearson correlation coefficient;
7. If PCC = 0.99 go to 8, if not go back to 4 with revising the parameters of network;
8. Continue processing until obtaining desired convergence between experimental and predicted values;
9. Obtain weights & biases values;
10. Create the model function;
11. Conduct analysis based on model function;
12. Verify the results using experimental values;
13. Calculate the error for each answer;
14. End.

4 RESULTS AND DISCUSSION

In order to train the ANNs in this study, the obtained experimental test results on shot peened (TiB + TiC)/Ti–6Al–4V composite specimens are employed. Different networks were trained to achieve the optimum structure (OS) in order to generate a model function (MF). After the OS is selected and the MF is generated, operation of the network is tested with the use of them (OS & MF). Twenty sample data (data of samples 1-20)

were used from the total of 30, as data sets for network training. **Table 3** shows the normalized sample data used for networks training. In the network testing, 10 different sample data (data of samples 21–30) which were not used during training are employed. Therefore, the whole experimental results did not comprise in the training. For investigative purposes, out of 30 samples data, 67 % data had taken for training and 33 % data for testing. Several networks have been trained with different architecture to find the OS of ANNs, to predict the regarded outputs, with the best performance and the highest PCC, the least RMSE, MRE and MAE. Related information of some the different trained networks for modelling of matrix hardness are shown in **Table 4**. The ordinal numbers shown in the "Layer Structure" were used to indicate the total number of neurons in the input, hidden and output layers, respectively. Results of the networks were investigated and the ANN modelling number 11 with 2×8×16×2 structure is selected for modelling and simulation.

Figures 4 and **5** show the obtained values of the ANN response in comparison with experimental values for each 20 training samples (samples 1–20) for residual stress and hardness, respectively, using the selected network.

After the network was trained, the selected network is tested. **Figures 6** and **7** have been demonstrated the predicted and experimental values of residual stress and hardness for 10 different testing samples (samples 21–30) respectively.

Table 3: Normalized sample data used for networks training
Tabela 3: Normalizirani podatki vzorca, uporabljenega pri usposabljanju mreže

Sample No.	Depth	SP intensity	Residual stress			Hardness		
			matrix	5 % (TIB+TIC)	8 % (TIB+TIC)	matrix	5 % (TIB+TIC)	8 % (TIB+TIC)
1	0.0000	0.0	0.0170	0.0277	0.0267	0.6377	0.6788	0.6552
2	0.0000	1.0	-0.8518	-0.8058	-0.8557	1.0000	1.0000	1.0000
3	0.0000	0.5	-0.6126	-0.6680	-0.7166	0.9227	0.9138	0.9170
4	0.0500	0.0	0.0409	0.0077	0.0102	0.6262	0.7024	0.6851
5	0.0500	1.0	-1.0000	-0.9970	-0.9781	0.8309	0.9140	0.9867
6	0.0500	0.5	-0.6803	-0.7678	-0.8024	0.7972	0.8795	0.8211
7	0.0833	0.0	-0.0156	-0.0311	-0.0193	0.6201	0.6804	0.6593
8	0.0833	1.0	-0.9917	-1.0000	-1.0000	0.7906	0.8356	0.8753
9	0.0833	0.5	-0.6663	-0.7158	-0.8547	0.7385	0.8058	0.7957
10	0.1667	0.0	0.0234	-0.0453	-0.0137	0.6009	0.7197	0.6461
11	0.1667	1.0	-0.9471	-0.9353	-0.9319	0.7214	0.8129	0.8329
12	0.1667	0.5	-0.6479	-0.6454	-0.8116	0.7098	0.7699	0.7456
13	0.2500	0.0	0.0236	0.0216	-0.0189	0.6445	0.6806	0.6648
14	0.2500	1.0	-0.9203	-0.8762	-0.8721	0.7342	0.7828	0.8448
15	0.2500	0.5	-0.5768	-0.5948	-0.7685	0.6826	0.7505	0.7008
16	0.3333	0.0	-0.0209	-0.0261	-0.0214	0.6478	0.7079	0.6503
17	0.3333	1.0	-0.9084	-0.8058	-0.7659	0.702	0.7737	0.7997
18	0.3333	0.5	-0.5291	-0.5188	-0.3930	0.6667	0.7341	0.7207
19	0.5000	0.0	-0.0086	-0.0182	-0.0129	0.6287	0.6704	0.6425
20	0.5000	1.0	-0.6882	-0.5160	-0.4447	0.6682	0.6937	0.6883

Table 4: Relevant information of 12 different networks for modeling of matrix hardness
Tabela 4: Pomembne informacije o 12 različnih mrežah pri modeliranju trdote osnove

ANN Modeling no.	Rate of training	Layers structure	Hidden transfer function	Output transfer function	PCC	RMSE	MRE (%)	MAE
1	0.090	2×2×4×2	Logsig	Linear	0.97035	0.7677	0.1552	0.6680
2	0.095	2×2×6×2	Tansig	Linear	0.97421	0.7018	0.1399	0.5742
3	0.110	2×2×8×2	Logsig	Tansig	0.98460	0.6671	0.1007	0.5018
4	0.100	2×4×4×2	Tansig	Linear	0.98662	0.4163	0.0938	0.4261
5	0.115	2×4×6×2	Logsig	Linear	0.99003	0.2397	0.0875	0.3459
6	0.120	2×4×10×2	Logsig	Linear	0.99150	0.2078	0.0617	0.2822
7	0.115	2×6×10×2	Tansig	Tansig	0.99877	0.3400	0.0587	0.2401
8	0.130	2×6×12×2	Tansig	Linear	0.99901	0.2229	0.0461	0.1886
9	0.145	2×6×16×2	Logsig	Tansig	0.99936	0.1997	0.0384	0.1597
10	0.160	2×8×10×2	Logsig	Logsig	0.99911	0.1609	0.0331	0.1529
11	0.165	2×8×16×2	Logsig	Logsig	0.99979	0.0985	0.0194	0.0853
12	0.165	2×8×20×2	Tansig	Linear	0.99963	0.1265	0.0247	0.1173

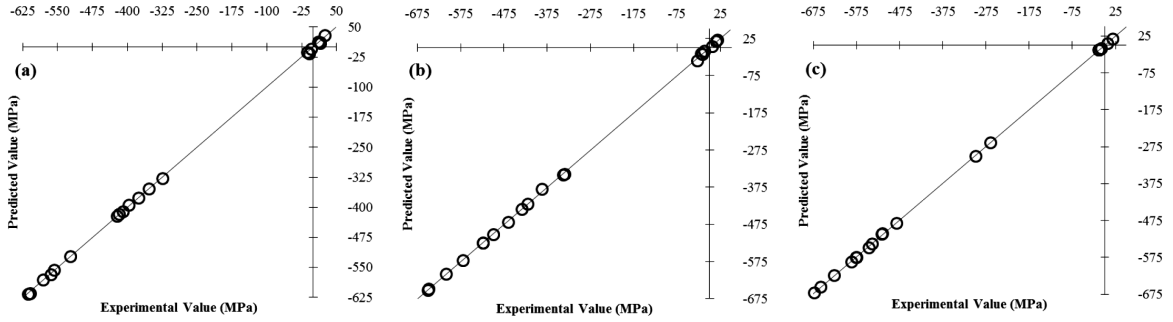

Figure 4: Comparison of predicted values (ANN response) with experimental values for each 20 training samples (samples 1–20) for residual stress: a) matrix, b) 5 % TiB+TiC and c) 8 % TiB+TiC

Figure 4: Primerjava napovedanih vrednosti (odgovor ANN) z eksperimentalnimi vrednostmi za vsakega od 20 vzorcev usposabljanja (vzorci 1-20) za zaostale napetosti: a) osnova, b) 5 % TiB+TiC in c) 8 % TiB+TiC

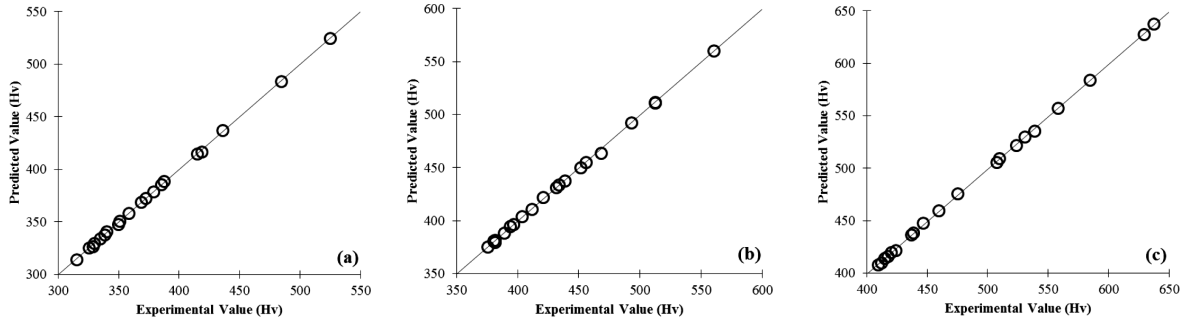

Figure 5: Comparison of predicted values (ANN response) with experimental values for each 20 training samples (samples 1–20) for hardness: a) matrix, b) 5 % TiB+TiC and c) 8 % TiB+TiC

Slika 5: Primerjava napovedanih vrednosti (odgovor ANN) z eksperimentalnimi vrednostmi za vsakega od 20 vzorcev usposabljanja (vzorci 1-20) za trdoto: a) osnova, b) 5 % TiB+TiC in c) 8 % TiB+TiC

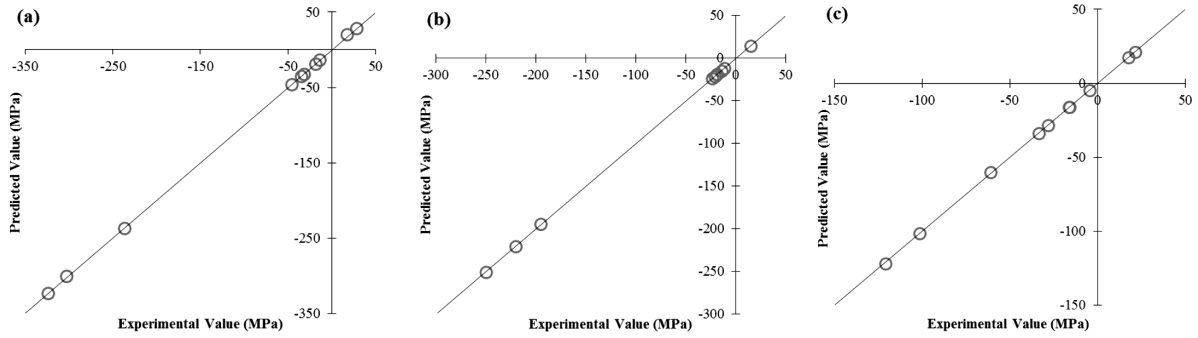

Figure 6: Comparison of predicted values (ANN response) with experimental values for each 20 testing samples (samples 21–30) for residual stress: a) matrix, b) 5 % TIB+TIC and c) 8 % TIB+TIC

Slika 6: Primerjava napovedanih vrednosti (odgovor ANN) z eksperimentalnimi vrednostmi za vsakega od 20 preizkušenih vzorcev (vzorci 21-30) za zaostale napetosti: a) osnova, b) 5 % TiB+TiC in c) 8 % TiB+TiC

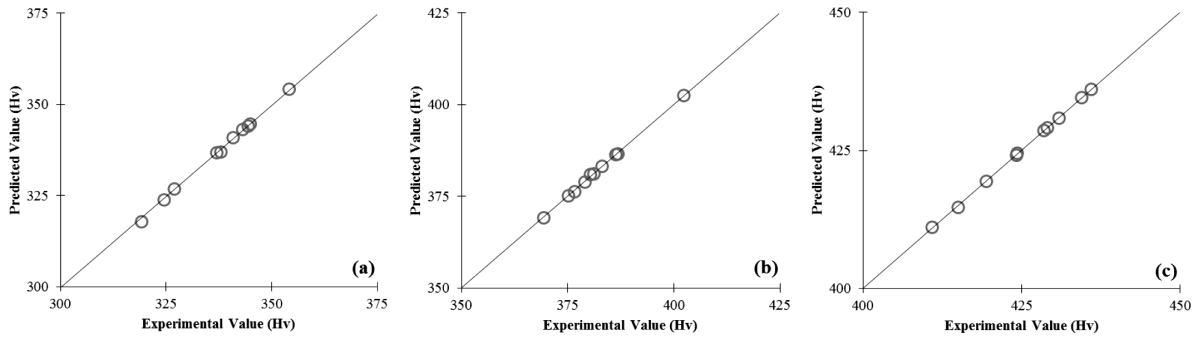

Figure 7: Comparison of predicted values (ANN response) with experimental values for each 20 testing samples (samples 21–30) for hardness: a) matrix, b) 5 % TIB+TIC and c) 8 % TIB+TIC

Slika 7: Primerjava napovedanih vrednosti (odgovor ANN) z eksperimentalnimi vrednostmi za vsakega od 20 preizkušenih vzorcev (vzorci 21-30) za trdoto: a) osnova, b) 5 % TiB+TiC in c) 8 % TiB+TiC

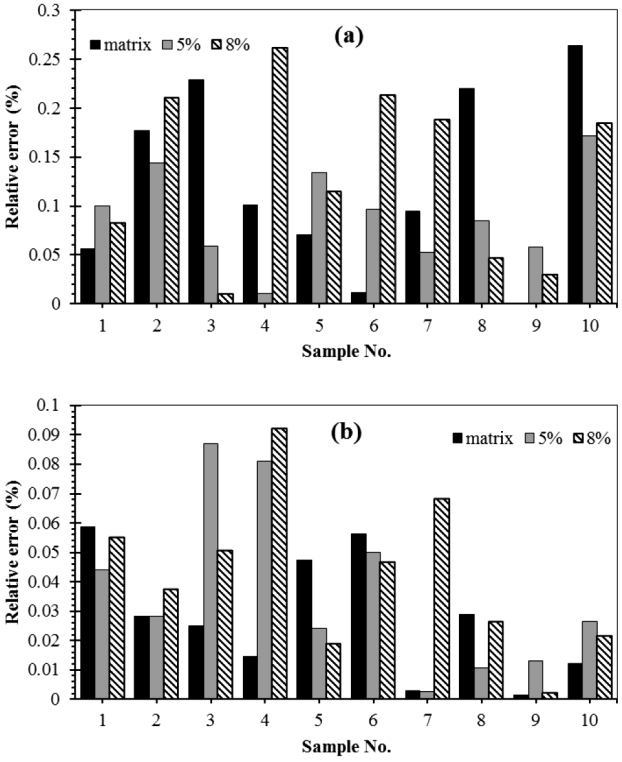

Figure 8: Values of obtained relative error for testing samples (samples 21–30) for considered output parameters: a) residual stress, b) hardness

Slika 8: Vrednosti dobljene relativne napake preizkušanih vzorcev (vzorci 21-30) pri upoštevanih izhodnih parametrih: a) zaostale napetosti, b) trdota

Figure 8 illustrates the obtained relative error (RE) values of the residual stress and hardness for the testing samples. In modeling of residual stress, according to the **Figure 8a**, the minimum and maximum (min., max.) determined relative errors for matrix, 5 % reinforcement and 8 % reinforcement are (0.000,0.2633), (0.0103, 0.1714) and (0.0099, 0.2616), respectively. Based on **Figure 8b**, similarly minimum and maximum calculated REs for matrix, 5 % reinforcement and 8 % reinforcement in modeling of hardness are (0.0015, 0.0587), (0.0026, 0.0870) and (0.0023, 0.0919), respectively.

According to the obtained values of the ANN for training and testing samples, data corresponding to the used network are shown in **Table 5**.

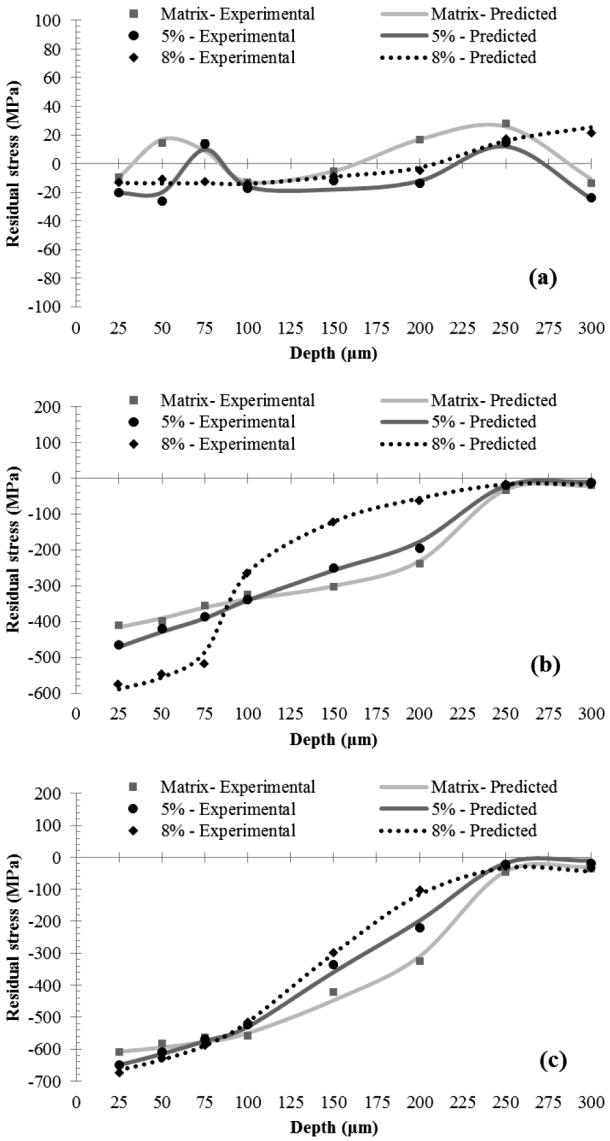

Figure 9: Distribution of residual stresses along the depth from the surface obtained by OS and MF of ANN for different SP intensities of: a) 0 mm A, b) 0.15 mm A and c) 0.3 mm A

Slika 9: Razporeditev spreminjanja zaostalih napetosti v globino od površine, dobljene pri OS in MF z ANN pri različnih intenzitetah SP: a) 0 mm A, b) 0,15 mm A in c) 0,3 mm A

In network training it is observed that the values of PCC for each considered output parameters are more than 99.7 %. The values of training RMSE, MRE and

Table 5: Obtained values of PCC, RMSE, MRE and MAE for trained and tested network

Tabela 5: Dobljene vrednosti PCC, RMSE, MRE in MAE pri usposobljeni in pri preizkušeni mreži

Output parameter		Training				Testing			
		PCC	RMSE	MRE (%)	MAE	PCC	RMSE	MRE (%)	MAE
Residual stress	Matrix	0.99914	0.1781	0.1104	0.1099	0.99846	0.2529	0.1223	0.1315
	5 % rein.	0.99875	0.0651	0.0872	0.0471	0.99816	0.0906	0.0910	0.0521
	8 % rein.	0.99766	0.0597	0.1228	0.0382	0.99683	0.0647	0.1342	0.0440
Hardness	Matrix	0.99979	0.0985	0.0194	0.0853	0.99912	0.1154	0.0276	0.0937
	5 % rein.	0.99901	0.1544	0.0313	0.1372	0.99858	0.1783	0.0368	0.1420
	8 % rein.	0.99837	0.1976	0.0346	0.1475	0.99721	0.2071	0.0419	0.1780

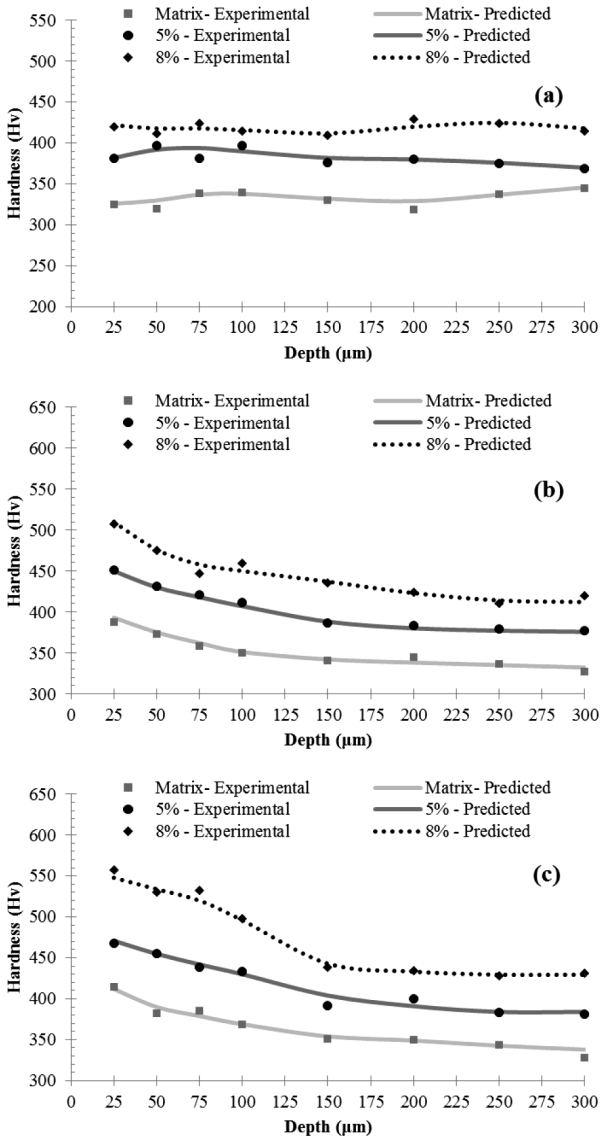

Figure 10: Distribution of hardness along the depth from the surface obtained by OS and MF of ANN for different SP intensities of: a) 0 mm A, b) 0.15 mm A and c) 0.3 mm A

Slika 10: Razporeditev vrednosti trdote v globino od površine, dobljene z OS in MF z AMM, pri različnih intenzitetah SP: a) 0 mm A, b) 0,15 mm A in c) 0,3 mm A

MAE are very close to 0 and they are in little intervals and their ranges are [0.0597, 0.1976], [0.0194, 0.1228] and [0.0382, 0.14715], respectively. So, it is concluded that networks are trained finely and adjusted carefully. Likewise in network testing the values of PCC are more than 99.6 % and it is observed that values of testing PCC have a negligible reduction in comparison with the training. Moreover, the values of testing RMSE, MRE and MAE are in a tiny span as well and their ranges are [0.0647, 0.2071], [0.0276, 0.1342] and [0.0440, 0.1780], respectively. Based on the achieved values for the statistical errors for both training and testing samples it is concluded that the error values are acceptable and implementation of ANN is accomplished in a good way.

In residual stress modeling for each case of network training and testing, the obtained values for 5 % TiB + TiC., matrix and 8 % TiB + TiC and in modeling of hardness, achieved values for matrix, 5 % TiB + TiC and 8 % TiB + TiC have the smallest errors, respectively. Distributions of the residual stress and hardness from the shot-peened surface to the bulk material (25-300 µm) for SP intensity of (0.00, 0.15 and 0.30) are shown in **Figures 9** and **10,** which are achieved by OS and MF of the used ANN modeling in this paper.

5 CONCLUSION

In present study the application of ANNs was investigated, aiming to create models to predict and optimize the SP process effects with different intensities on the residual stress and hardness of a (TiB + TiC)/Ti–6Al–4V composite. Experimental data show that both the residual stress and the hardness were increased with an improvement of the SP intensities. Residual stress and hardness were modeled using ANN for three cases: matrix, 5 % TiB + TiC and 8 % TiB + TiC. The obtained results indicate that statistical errors for RSME, MRE and MAE are in very small range and so close to 0. Moreover, the values of PCC for all of the regarded output parameters in implemented networks are more than 99 %. According to the achieved results, it can be concluded that when the ANNS are tuned in a good way and adjusted carefully, the modeling results are in reasonable agreement with the experimental results. Therefore, using ANNs, instead of costly and time consuming experiments, decreases the costs and the need for special testing facilities, and the ANNs can be employed to predict and optimize the SP effects on the residual stress and the hardness of TMCs.

6 REFERENCES

[1] S. C. Tjong, Z. Ma, Microstructural and mechanical characteristics of in situ metal matrix composites, Materials Science and Engineering: R: Reports, 29 (**2000**), 49–113, doi:10.1016/S0927-796X(00)00024-3

[2] S. C. Tjong, Y. W. Mai, Processing-structure-property aspects of particulate-and whisker-reinforced titanium matrix composites, Composites Science and Technology, 68 (**2008**), 583–601, doi:10.1016/j.compscitech.2007.07.016

[3] L. Huang, L. Geng, H. Peng, In situ (TiBw+ TiCp)/Ti6Al4V composites with a network reinforcement distribution, Materials Science and Engineering A, 527 (**2010**), 6723–6727, doi:10.1016/j.msea.2010.07.025

[4] A. Mavi, I. Korkut, Machinability of a ti-6al-4v alloy with cryogenically treated cemented carbide tools, Mater. Tehnol., 48 (**2014**), 577–580

[5] W. Lu, D. Zhang, X. Zhang, R. Wu, T. Sakata, H. Mori, HREM study of TiB/Ti interfaces in a TiB-TiC in situ composite, Scripta Materialia, 44 (**2001**), 1069–1075, doi:10.1016/S1359-6462(01)00663-7

[6] H. Man, S. Zhang, F. Cheng, T. Yue, Microstructure and formation mechanism of in situ synthesized TiC/Ti surface MMC on Ti-6Al-4V by laser cladding, Scripta Materialia, 44 (**2001**), 2801–2807

[7] W. Lu, D. Zhang, X. Zhang, Y. Bian, R. Wu, T. Sakata, H. Mori, Microstructure and tensile properties of in situ synthesized (TiBw+ TiCp)/Ti6242 composites, Journal of Materials Science, 36 (**2001**), 3707–3714, doi:10.1023/A:1017917631855

[8] B. Li, J. Shang, J. Guo, H. Fu, In situ observation of fracture behavior of in situ TiB w/Ti composites, Materials Science and Engineering A, 383 (**2004**), 316–322, doi:10.1016/j.msea.2004.04.071

[9] T. Saito, T. Furuta, T. Yamaguchi, Development of low cost titanium alloy matrix composite, Recent Advances in Titanium Metal Matrix Composites, (**1994**), 33–44

[10] Z. Wei, L. Cao, H. Wang, C. Zou, Microstructure and mechanical properties of TiC/Ti-6Al-4V composites processed by in situ casting route, Materials Science and Technology, 27 (**2011**), 1321–1327, doi:10.1179/026708310X12699498462922

[11] M. Y. Koo, J. S. Park, M. K. Park, K. T. Kim, S. H. Hong, Effect of aspect ratios of in situ formed TiB whiskers on the mechanical properties of TiB w/Ti–6Al–4V composites, Scripta Materialia, 66 (**2012**), 487–490, doi:10.1016/j.scriptamat.2011.12.024

[12] H. Rastegari, S. Abbasi, Producing Ti–6Al–4V/TiC composite with superior properties by adding boron and thermo-mechanical processing, Materials Science and Engineering A, 564 (**2013**), 473–477, doi:10.1016/j.msea.2012.12.011

[13] S. Ranganath, M. Vijayakumar, J. Subrahmanyan, Combustion-assisted synthesis of Ti-TiB-TiC composite via the casting route, Materials Science and Engineering A, 149 (**1992**), 253–257, doi:10.1016/0921-5093(92)90386-F

[14] X. Zhang, W. Lü, D. Zhang, R. Wu, Y. Bian, P. Fang, In situ technique for synthesizing (TiB+ TiC)/Ti composites, Scripta Materialia, 41 (**1999**), 39–46, doi:10.1016/S1359-6462(99)00087-1

[15] M. M. Wang, W. J. Lu, J. N. Qin, D. Zhang, B. Ji, F. Zhu, Superplastic behavior of in situ synthesized (TiB+ TiC)/Ti matrix composite, Scripta Materialia, 53 (**2005**), 265–270, doi:10.1016/j.scriptamat.2005.01.049

[16] J. Lu, J. Qin, W. Lu, Y. Chen, D. Zhang, H. Hou, Effect of hydrogen on superplastic deformation of (TiB+ TiC)/Ti–6Al–4V composite, International Journal of Hydrogen Energy, 34 (**2009**), 8308–8314, doi:10.1016/j.ijhydene.2009.07.091

[17] S. Sun, M. Wang, L. Wang, J. Qin, W. Lu, D. Zhang, The influences of trace TiB and TiC on microstructure refinement and mechanical properties of in situ synthesized Ti matrix composite, Composites Part B: Engineering, 43 (**2012**), 3334–3337, doi:10.1016/j.compositesb.2012.01.075

[18] M. M. Wang, W. J. Lu, J. Qin, F. Ma, J. Lu, D. Zhang, Effect of volume fraction of reinforcement on room temperature tensile property of in situ (TiB+ TiC)/Ti matrix composites, Materials & Design, 27 (**2006**), 494–498, doi:10.1016/j.matdes.2004.11.030

[19] W. Lu, D. Zhang, X. Zhang, R. Wu, T. Sakata, H. Mori, Microstructure and tensile properties of in situ (TiB+ TiC)/Ti6242 (TiB: TiC= 1: 1) composites prepared by common casting technique, Materials Science and Engineering A, 311 (**2001**), 142–150, doi:10.1016/S0921-5093(01)00910-8

[20] B. R. Bhat, J. Subramanyam, V. B. Prasad, Preparation of Ti-TiB-TiC & Ti-TiB composites by in-situ reaction hot pressing, Materials Science and Engineering A, 325 (**2002**), 126–130, doi:10.1016/S0921-5093(01)01412-5

[21] D. Ni, L. Geng, J. Zhang, Z. Zheng, Fabrication and tensile properties of in situ TiBw and TiCp hybrid-reinforced titanium matrix composites based on Ti–B 4 C–C, Materials Science and Engineering A, 478 (**2008**), 291–296, doi:10.1016/j.msea.2007.06.004

[22] M. Khayet, C. Cojocaru, M. Essalhi, Artificial neural network modeling and response surface methodology of desalination by reverse osmosis, Journal of Membrane Science, 368 (**2011**), 202–214, doi:10.1016/j.memsci.2010.11.030

[23] L. Xie, C. Jiang, W. Lu, The influence of shot peening on the surface properties of (TiB+ TiC)/Ti–6Al–4V, Applied Surface Science, 280 (**2013**), 981–988, doi:10.1016/j.apsusc.2013.05.135

[24] M. T. Ozkan, H. B. Ulas, M. Bilgin, Experimental design and artificial neural network model for turning the 50crv4 (sae 6150) alloy using coated carbide/cermet cutting tools, Mater. Tehnol., 48 (**2014**), 227–236

[25] A. Mukherjee, S. Schmauder, M. Ru, Artificial neural networks for the prediction of mechanical behavior of metal matrix composites, Acta metallurgica et materialia, 43 (**1995**), 4083–4091, doi:10.1016/0956-7151(95)00076-8

[26] J. Han, M. Kamber, Data mining: concepts and techniques, 2nd Ed., Amsterdam, 2006

[27] D. Afshari, M. Sedighi, M. R. Karimi, Z. Barsoum, Prediction of the nugget size in resistance spot welding with a combination of a finite-element analysis and an artificial neural network, Mater. Tehnol., 48 (**2014**), 33–38

[28] U. Özdemir, B. Özbay, S. Veli, S. Zor, Modeling adsorption of sodium dodecyl benzene sulfonate (SDBS) onto polyaniline (PANI) by using multi linear regression and artificial neural networks, Chemical Engineering Journal, 178 (**2011**), 183–190, doi:10.1016/j.cej.2011.10.046

[29] A. Çelekli, S. S. Birecikligil, F. Geyik, H. Bozkurt, Prediction of removal efficiency of Lanaset Red G on walnut husk using artificial neural network model, Bioresource technology, 103 (**2012**), 64–70, doi:10.1016/j.biortech.2011.09.106

[30] M. Rezakazemi, S. Razavi, T. Mohammadi, A. G. Nazari, Simulation and determination of optimum conditions of pervaporative dehydration of isopropanol process using synthesized PVA–APTEOS/TEOS nanocomposite membranes by means of expert systems, Journal of Membrane Science, 379 (**2011**), 224–232, doi:10.1016/j.memsci.2011.05.070

[31] M. Rezakazemi, T. Mohammadi, Gas sorption in H 2-selective mixed matrix membranes: Experimental and neural network modeling, International Journal of Hydrogen Energy, 38 (**2013**), 14035–14041, doi:10.1016/j.ijhydene.2013.08.062

[32] L. Wang, B. Yang, R. Wang, X. Du, Extraction of pepsin-soluble collagen from grass carp (Ctenopharyngodon idella) skin using an artificial neural network, Food Chemistry, 111 (**2008**), 683–686, doi:10.1016/j.foodchem.2008.04.037

[33] E. Maleki, K. Sherafatnia, Investigation of single and dual step shot peening effects on mechanical and metallurgical properties of 18CrNiMo7-6 steel using artificial neural network, International Journal of Materials, Mechanics and Manufacturing, 4 (**2016**), 100–105, doi:10.7763/IJMMM.2016.V4.233

[34] S. Haykin, N. Network, A comprehensive foundation, Neural Networks, 2 (**2004**)

[35] T. P. Vogl, J. Mangis, A. Rigler, W. Zink, D. Alkon, Accelerating the convergence of the back-propagation method, Biological cybernetics, 59 (**1988**), 257–263, doi:10.1007/BF00332914

[36] A. Savran, M. Alci, S. Yildirim, R. Yigit, E. Celik, Application of a neural network for estimating the crack formation and propagation in sol-gel CeO_2 coatings during processing at temperature, Mater. Tehnol., 48 (**2014**), 453–457

[37] P. Shabanzadeh, N. Senu, K. Shameli, F. Ismail, M. Mohagheghtabar, Application of artificial neural network (ANN) for the prediction of size of silver nanoparticles prepared by green method, Digest Journal of Nanomaterials and Biostructures, 8 (**2013**), 541–549